Evaluation of WEDM performance characteristics of Inconel 706 for turbine disk application

Priyaranjan Sharma, D. Chakradhar, S. Narendranath

PII: S0264-1275(15)30445-7
DOI: doi: 10.1016/j.matdes.2015.09.036
Reference: JMADE 606

To appear in:

Received date: 21 July 2015
Revised date: 7 September 2015
Accepted date: 8 September 2015

Please cite this article as: Priyaranjan Sharma, D. Chakradhar, S. Narendranath, Evaluation of WEDM performance characteristics of Inconel 706 for turbine disk application, (2015), doi: 10.1016/j.matdes.2015.09.036

Evaluation of WEDM performance characteristics of Inconel 706 for turbine disk application

Priyaranjan Sharma*, D. Chakradhar, Narendranath S.

Department of Mechanical Engg., National Institute of Technology Karnataka, Surathkal - 575025, India.

Email id: priya333ranjan@nitk.edu.in

Abstract

Inconel 706 is a newly developed superalloy, which offers high mechanical strength along with easy fabricability thus making it suitable for turbine disk applications. Although Inconel 706 exhibits a substantial increase in stress rupture and tensile yield strength compared to other superalloys, its conventional machining yields poor surface finish and low dimensional accuracy of the machined components. Hence, wire electrical discharge machining (WEDM) of Inconel 706 has been performed and various performance attributes such as material removal rate (MRR), surface roughness (SR), recast surface, topography, microhardness, microstructural and metallurgical changes of the machined components have been evaluated. The experimental results revealed that servo voltage, pulse on time, and pulse off time greatly influence the MRR and SR. Due to high toughness of Inconel 706, no micro cracks were observed on the machined surface. Micro voids and micro globules are significantly reduced at low pulse on time and high servo voltage. But, there is a propensity of thick recast layer formation at high pulse on time and low servo voltage. EDAX analysis of recast surface exposed the existence of Cu and Zn which have migrated from brass wire. The subsurface microhardness was changed to 80 µm due to significant thermal degradation.

Keywords: Inconel 706; WEDM; topography; Microstructure; Microhardness; EDAX.

1. Introduction

In the recent times, machining of nickel-iron-based superalloys has become an active area of research due to its growing demand in aircraft turbines, rocket engines, power generation turbines, nuclear plants, chemical treatment plants and other challenging environments. These superalloys exhibit outstanding properties such as high toughness and ductility, good surface stability, creep resistance at high temperature, corrosion and oxidation resistance [1]. Therefore, their usage has vital importance in designing of high performance gas turbine engines [2]. Due to the requirement of high temperature and compressor ratio for advance gas turbine engines, it became necessary to utilize a newly developed superalloy [3]. Inconel 706 is one of the advance superalloy and specially developed for aircraft applications, particularly in manufacturing for turbine disks, diffuser cases, compressor disks, engine mounts, and fasteners. Since this alloy is not much prone to segregation, it could be used to fabricate enormous components and make it ideal for the manufacturing of gas turbine components. Conventional machining of nickel-iron-based superalloys include several issues, such as poor surface quality, low dimensional accuracy, high tool wear rate, and poor machinability [4].

These issues are commonly observed because of their high abrasive nature, high work-hardening tendency and high chemical affinity.

To overcome these issues, non-traditional machining processes such as laser beam machining (LBM), abrasive water jet machining (AWJM), electrochemical machining (ECM), electrical discharge machining (EDM) and wire electrical discharge machining (WEDM) could be successfully implemented to process these superalloys. Among these processes, WEDM provides higher flexibility in cutting the complex shapes with high precision and is highly suitable for the manufacturing of gas turbine components. In addition, WEDM requires less cutting force in material removal and offers low residual stresses in the machined components. Previous studies revealed that WEDM exhibits good strength of the components compared to the conventional broaching process while manufacturing the fir tree slots through the turbine disk [5]. In order to increase the productivity of WEDM process, Klocke *et al.* [6] developed the machining technology for the manufacturing of fir tree slots in Inconel 718. With the usage of coated high speed cutting wire, manufacturing time has been reduced by 33%, while the best surface integrity of the machined components has been achieved using standard brass wire. Up to 40% increase in productivity and 25% thinner recast layer were achieved using coated wire during the WEDM process of Udimet 720 [7]. Further, Klocke *et al.* [8] developed the process monitoring tool to correlate the surface integrity of the WEDM process for fir tree slot production. Atzeni *et al.* [9] evaluated the surface and subsurface alteration of WED machined surface of Inconel 718. With the appropriate settings of discharge energy and wire feed rate, no thermal modifications were observed on machined surfaces.

During the WEDM of Inconel 718, minimum level of workpiece damage was obtained using the modified generator technology, which also exposed that there is no significant change in microhardness of the machined components with cracking limited to recast layer. With the usage of several trim passes, no apparent recast layer was detected on the machined surface [10]. The recast layer formed on the WED machined components is highly undesirable for the aerospace application. Further, Newton *et al.* [11] investigated the recast layer formation and its characteristics during the WEDM process of Inconel 718. They found that the average recast layer thickness was within the range of 5 to 9 µm. The recast material had lower hardness as well as lower elastic modulus compared to the base material. The surface topography of the WED machined surface exposed coral reef microstructure at high pulse energy, but reduced micro voids at low pulse energy. Li *et al.* [12] have exposed that micro voids were limited within a thick white layer, but no micro cracks were observed on the subsurface. Thick white layer was mostly discontinuous and non-uniform at high pulse energy. Under trim cut mode, this white layer became nearly invisible and no microcracks were observed due to high toughness of Inconel 718 [13].

In order to prevent the fatigue failure of aeroengine components, fatigue performance of WED machined Udimet 720 have been studied by Antar *et al.* [14] using minimum damage generator technology. No microcracks were detected on the WED machined surface using trim cuts employing low discharge energy thus resulting in improved fatigue performance. Looking into continuous improvement in surface quality of aerogine components, the current

study has been carried out to evaluate the WEDM performance of Inconel 706 for turbine disk application where complex shape profiles along with high surface quality are desired.

Other than the surface integrity evaluation of WED machined components of nickel-based superalloy, some researchers have developed the mathematical model to correlate the interrelationships between WEDM control parameters (i.e., peak current, duty factor, wire tension and water pressure) and machining characteristics (MRR, SR, and wear ratio) while machining Inconel 601. It was reported that the MRR increased to 8 mm^3/min and SR reduced to 0.8 µm [15]. To predict the optimum machining characteristics of WEDM process during the cutting of Inconel 718, artificial neural network (ANN) model was established using back-propagation algorithms. It was observed that the ANN model with an optimization tool predicts the WEDM control parameters more effectively, which might be beneficial to the manufacturing communities [16]. It is a matter of fact that WEDM has a random mechanism of material removal and there is a significant role of control parameters to improve the productivity as well as surface quality of the component.

Even though, WEDM has publicized the good capability of cutting the complex shape profile through the conductive components required for specific applications, the surface quality of the newly developed superalloy components is poorly reviewed. Particularly, not many literatures are available regarding the investigation of surface characteristics of Inconel 706 superalloy in WEDM process. Due to the high quality requirement of gas turbine components such as negligible recast layer, zero porosity, normal residual stress, absence of cracks and recrystallized zone, still there is a necessity to evaluate the WEDM performance characteristics while cutting complex shape profile through Inconel 706. Present work reports on the experimental investigation of WEDM performance characteristics such as MRR, SR, recast layer thickness (RLT), microhardness, surface topography and microstructure of the machined components.

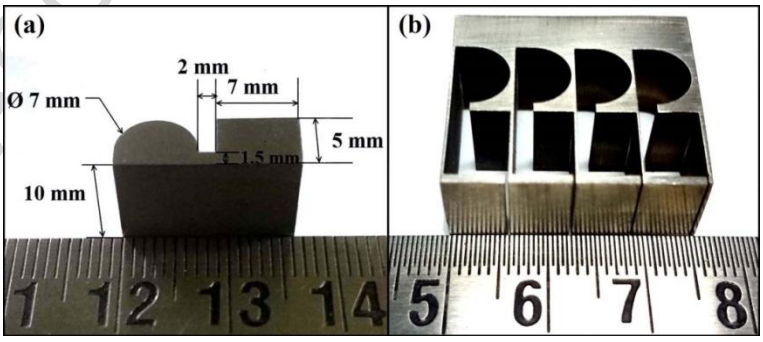

Fig. 1. Profile of WED machined component of Inconel 706 (a); Profile slot obtained after WEDM process (b).

2. Materials and methods

2.1 Material selection

Inconel 706 was selected as a target material which is a newly developed nickel-iron-based superalloy as a substitute of Inconel 718 for turbine disk application. The chemical composition of as-received Inconel 706 has been presented in Table 1. The superalloy was procured in the form of plate (200 mm × 200 mm × 10 mm) from 'Special Metals', India. The properties of Inconel 706 are almost similar to Inconel 718 except their lower percentage

of alloying elements and good fabricability. Some physical and mechanical properties of Inconel 706 have been listed in Table 2. Molybdenum, which is existing in Inconel 718, is excluded from Inconel 706 to improve forgability and niobium content was reduced to decrease the affinity of freckle formation and segregation [17].

Table 1. Chemical composition of as-received Inconel 706 [18].

Alloy (%)		Ni+Co	Cr	Fe	Nb+Ta	Ti	Co	C	Mn	Si	S	Cu	Al	P
Inconel 706	Min.	39	14.5	Bal	2.5	1.5								
	Max.	44	17.5		3.3	2	1	0.06	0.35	0.35	0.02	0.3	0.4	0.02

Table 2. Physical and mechanical properties of Inconel 706 [18].

Properties of Inconel 706	Specification
Density	8.05 g/cm³
Melting range	1334-1371°C
Thermal conductivity	12.5 W/mK
Modulus of elasticity	210 kN/mm^2
Tensile strength	1282 MPa
Yield strength (0.2% offset)	993 MPa
Elongation	19%

The alloy was stress relieved prior to the WEDM operation to avoid distortion and to ensure minimum residual stresses. To attain that, all the specimens were heated to a temperature of 800°C in a tubular furnace for 1 hour and then cooled down at room temperature.

2.2 Experimental details

The experiments were performed on 'ELECTRONICA ECOCUT' WED machine. The WED machine has two distinct options as it can be operated either in power pulse mode (pulse current of 12 A) or fine pulse mode (pulse current of 1 A). Generally, the power pulse mode is used for basic cutting operation while fine pulse mode is used for finishing operation of machined surface.

Table 3. Control parameters and their levels.

Control parameters	Level-1	Level-2	Level-3	Level-4	Level-5
Pulse on time (μs)	105	110	115	120	125
Pulse off time (μs)	18	27	36	45	54
Servo voltage (V)	20	35	50	65	80
Wire feed (m/min)	2	4	6	8	10
Servo feed (mm/min)	5	10	15	20	25
Flushing pressure (bar)	1.37	1.67	1.96	2.25	2.55

In the current study, efforts have been made to investigate the effect of WEDM control parameters on performance characteristics using power pulse mode. Six control parameters, namely, pulse on time, pulse off time, servo voltage, servo feed, wire feed and flushing pressure were identified and the range of control parameters was estimated through preliminary trials. In the range of parameters selected, no wire breakage and gap short problem were recorded. The control parameters and their levels have been shown in Table 3. All the control parameters have been examined at five different levels to study the linear/non-linear effect of control parameters with respect to the machining characteristics (i.e. MRR,

SR). One factor at a time (OFAT) approach has been proposed for the current investigation in which one factor was varied at one time and other factors were maintained at their average level (Level-3). This approach helped to determine the individual effect of each control parameter on the machining characteristics. Based on the machine performance stability, some control parameters were kept constant throughout the experimental work as shown in Table 4.

Table 4. Constant process parameters used during the WEDM process.

Wire diameter	250 μm
Wire material	Standard brass
Dielectric fluid	De-ionized water
Polarity	Positive
Peak current	12 A
Peak voltage	11 V
Current Speed (%)	50
Dwell time	3 μs
Corner control factor	3

The standard brass wire was selected as the tool electrode because this wire offers the best surface integrity of the machined components compared to the coated wire [7]. Fig. 1(a) shows the complex profile of the WED machined component of Inconel 706, The complex profile slot obtained after the machining of Inconel 706 has been shown in Fig. 1(b).

2.3 Measurement of performance characteristics

The material removal rate (MRR) has been determined using the weight loss method and computed as follows:

$$MRR = \frac{(Wi\text{-}Wf)}{\rho \times t} \quad (1)$$

Where,

Wi = Weight of the specimen before machining (g),
Wf = Weight of the specimen after machining (g),
ρ = Density of the specimen (g/mm^3), and
t = Machining time (sec).

Each specimen was weighed using a digital weighing balance having an accuracy of 0.0001 g. Before weighing, each specimen was dried using a hot air blower to remove the moisture. The machining time was calculated using digital stopwatch. The surface roughness (SR) of the WED machined components were measured using 'Surftest SJ-301' surface roughness tester. Here, average surface roughness (Ra), which is normally used in manufacturing industries, is considered for the current investigation. The SR of each specimen was measured at five altered places and their average was taken as the final response.

The surface topography was measured using 'LEST OLS4100' 3D laser microscope, which uses laser scanning to measure the surface profile of the machined components. The microstructure graph of as-received and machined specimen was obtained using 'JEO JSM-638OLA' scanning electron microscope (SEM) to study the surface morphology. For SEM analysis, as-received and WED machined specimens were polished using SiC papers to

remove the scratches. Finally, diamond polishing was done to obtain mirror finish on the specimen. Marble's reagent (10 g $CuSO_4$ + 50 ml HCl + 50 ml H_2O + few drops of H_2SO_4) was used to etch the polished specimen of Inconel 706 superalloy. The etching time of the specimens was kept around 110 to 120 sec. To study the recast surface, the cross-section of the WED machined component was mirror polished. Then, SEM images were taken to analyze the recast layer formation.

The microhardness of the cross-section of WED machined surface was measured using 'OMNI TECH MVH-S-AUTO' micro Vickers hardness tester. Prior to microhardness measurement, the cross-section of machined sample was kept upward before being cold mounted using acrylic powder and self curing liquid. Then, cold mounted samples were mirror polished to obtain the perfect indentation mark. The microhardness was measured at 10 kgf load with dwell time of 10 sec. The expression [19] used to calculate the microhardness is expressed as follows:

$$\mathrm{Hv} = \frac{2F\sin\frac{136^{o}}{2}}{d^{2}} = 1.854\frac{F}{d^{2}} \qquad (2)$$

Where,

Hv = Vicker hardness,

F = Applied load and

d = Mean of two diagonals of a squared pyramid having an angle of 136°.

3. Results and discussion

3.1 Microstructure properties of as-received Inconel 706

Fig. 2(a) shows the SEM image of Inconel 706 superalloy which shows the fine and stable equi-axed grains. The grain size analysis was done using BIOVIS software as per the ASTM E112 standard which uses the liner intercept method. The grain size of the polished Inconel 706 specimen was found to be 13.50 µm. The elemental composition of as-received Inconel 706 has been confirmed by EDAX analysis as shown in Fig. 2(b). The alloy contains both niobium and aluminium and is strengthened by a combination of second precipitate phase (γ') and hard secondary phase (γ'') [20]. The microstructure also shows the formation of γ" (Ni_3Nb).

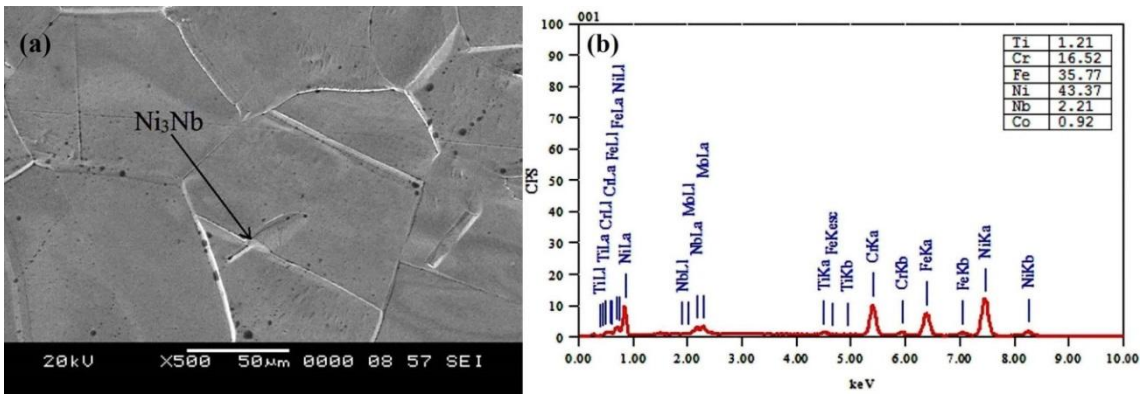

Fig. 2. Microstructure of as-received Inconel 706 (a); and EDAX analysis of Inconel 706 (b).

3.2 Analysis of material removal rate

The variation of MRR with respect to the control parameters (i.e., pulse on time, pulse off time, servo voltage, servo feed, wire feed, flushing pressure) has been shown in Fig. 3. From the Fig. 3(a), it was observed that MRR increases with increased pulse on time, whereas MRR decreases with increased servo voltage and pulse off time. This behavior can be explained by the fact that at high pulse on time, the intensity of the spark will increase, which in turn removes comparatively more amount of material from the sparking zone resulting in high MRR. Moreover, MRR decreases with increased in pulse off time as shown in Fig. 3(b). This is due to reduced number of sparks in specified time, which in turn, reduces the size of the crater formed on the machined surface leading to lower MRR.

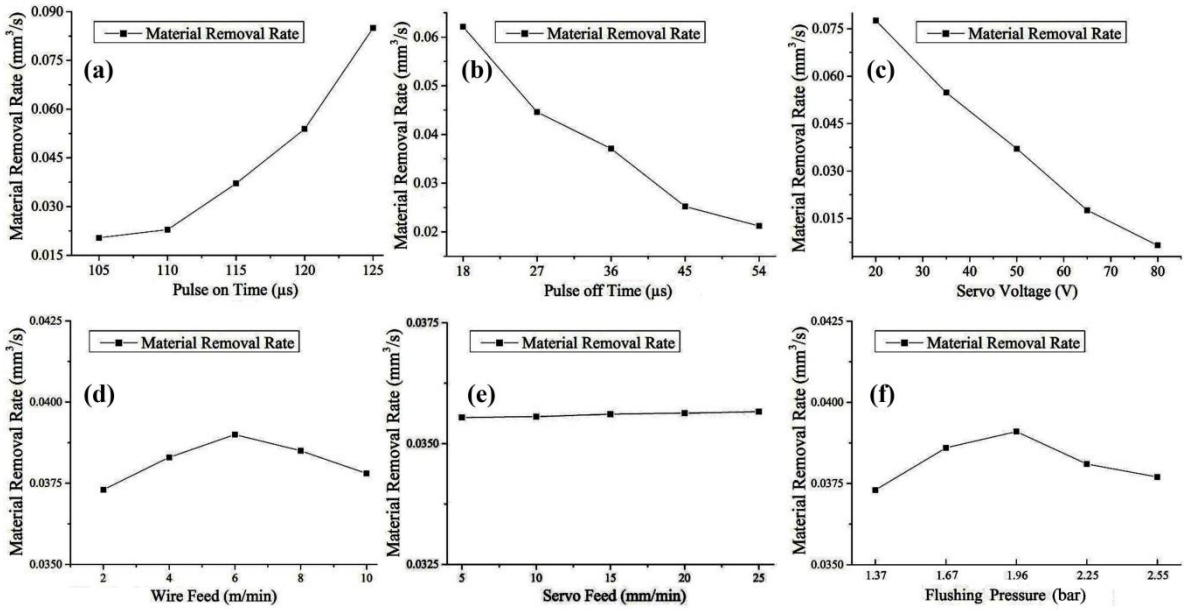

Fig. 3. Effect of control parameters on MRR.

Fig. 3(c) shows that MRR decreases with increase in servo voltage. That's because, at high servo voltage, the average spark gap gets widened and thus reduces the spark intensity leading to lower MRR. Consequently, less material will be melted resulting in lower MRR. From the Fig. 3(d), it was observed that an increase in wire feed upto 6 m/min, more amount of molten material splashed through the machining zone and hence leading to higher MRR. At higher wire feed of more than 6 m/min, wire vibration comes into play that reduces the dynamic stability of wire and causes the unfavorable sparking condition and hence leading to lower MRR.

From Fig. 3(e), it was observed that MRR almost remains constant for all the specified levels of servo feed. The MRR increases with the increase in flushing pressure up to 1.96 bar and thereafter it decreases as shown in Fig. 3(f). Since, an increase in flushing pressure leads to spilling out the relatively more amount of molten material thus leading to higher MRR. The high flushing pressure (more than 1.96 bar) causes the unfavorable sparking conditions due to wire deflection and wire vibration [21] thus affecting the spark intensity which leads to lower MRR.

3.3 Analysis of surface roughness

The effect of various control factors on SR has been shown in Fig. 4. From Fig. 4(a), it was observed that SR increases with increased pulse on time because at high pulse on time, the intensity of the spark will increase, which in turn induces the deeper and larger crater into the workpiece resulting to higher SR. Fig. 4(b) shows the reduced SR at high pulse off time. That's because, at high pulse off time, cooling time will increase, which also increases the flushing time, which tends to spilling out of comparatively more amount of molten material through the machining zone and hence reduces the SR. Our investigation revealed that SR is drastically reduced with an increase in servo voltage as shown in Fig. 4(c). That's because, an increase in servo voltage tends to widen the spark gap. Therefore, it reduces the spark intensity and increases the flushing and thus forms micro cavities on the machined surface leading to better surface quality.

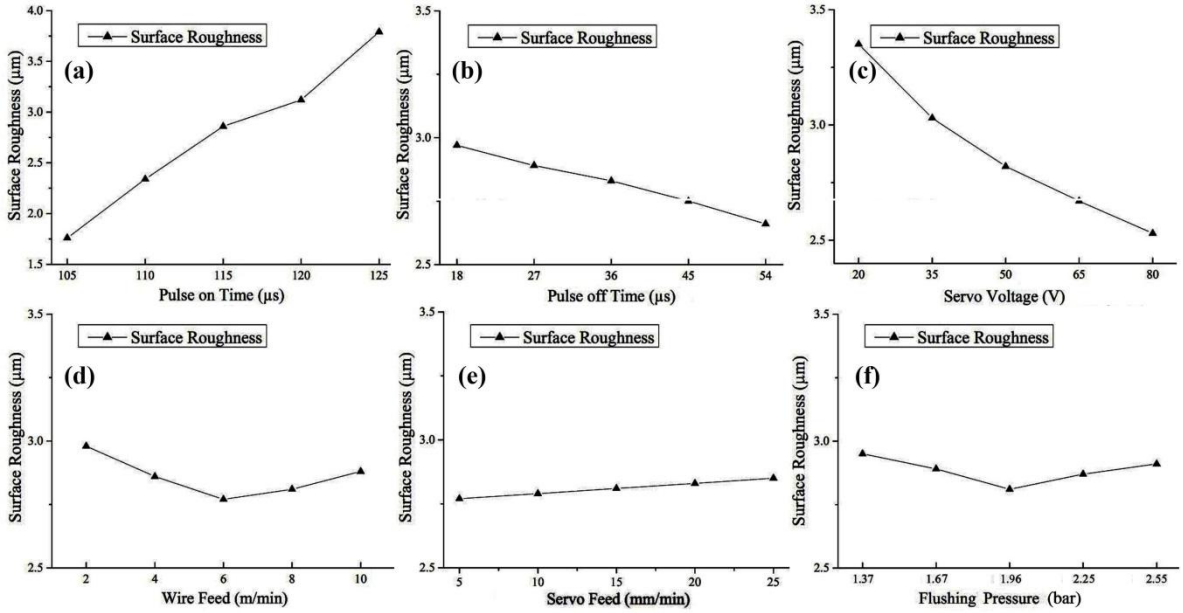

Fig. 4. Effect of control parameters on SR.

Fig. 4(d) and Fig. 4(f) have shown an almost similar trend of SR with increased wire feed and flushing pressure. It was evident from Fig. 4(d) that SR decreases with an increase in wire feed upto 6 m/min, beyond that SR increases. This behavior can be explained by the fact that at a higher wire feed upto 6 m/min, SR gets reduced due to improved splashing of molten material. However, beyond 6 m/min, it was observed that SR increases because wire vibration comes into play. This will cause unfavorable sparking conditions and thus creates uneven craters on the machined surface which leads to higher SR. Fig. 4(e) indicates that there is no more variation in SR at specified levels of servo feed. From Fig. 4(f), it was observed that low flushing pressure enhances the contamination of dielectric fluid and contributes to unfavorable sparking conditions leading to higher SR. The SR decreases with increased flushing pressure up to 1.96 bar and thereafter it increases. Since, an increase in flushing pressure leads to spilling out of relatively more amount of molten material and reduces the formation of micro voids on the machined surface leading to lower SR. The higher flushing pressure (more than 1.96 bar) again contributes to the unfavorable sparking

conditions and thus create uneven craters on the machined surface leading to higher SR. Past studies [21] revealed that high flushing pressure leads to more wire deflection and contributes to the wire vibration. Thus, it affects the shape accuracy of the machined components as well as SR and increases the chances of wire breakage.

3.4 Analysis of surface topography

The surface topography of the WED machined surface has been shown in Fig. 5. From topography analysis, it was revealed that servo voltage and pulse on time are the major factors affecting the surface quality of the machined components.

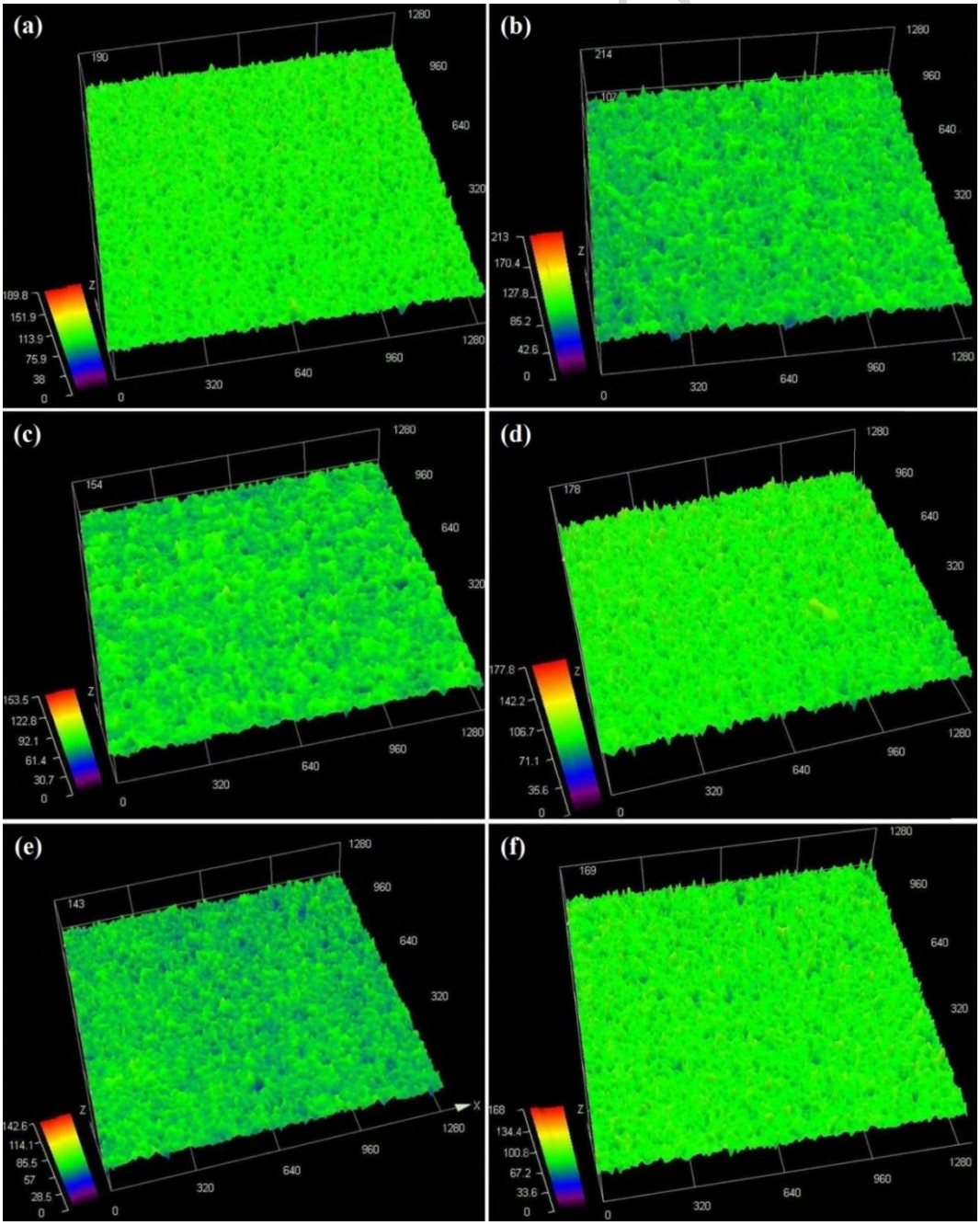

Fig. 5. Surface topography of WED machined surface under the following machine setting: (a) pulse on time of 105 µs; (b) pulse on time of 125 µs; (c) servo voltage of 20 V; (d) servo voltage of 80 V; (e) pulse off time 18 µs; (f) pulse on time 54 µs.

Higher smoothness and fine surface can be obtained at low pulse on time of 105 µs because of low pulse intensity as shown in Fig. 5(a). On the other hand, the high intensity sparks form larger and deeper crater on the machined surface and hence, offering a rough surface as shown in Fig. 5(b). After comparing the average SR of the machined components at pulse on time of 105 µs and 125 µs, the difference of 2.03 µm has been found which indicates that pulse on time has great influence on the SR of the machined components. Similarly, by comparing the average SR of the machined components at servo voltage of 20 V and 80 V, the difference of 0.73 µm has been observed which indicates that servo voltage is the other significant factor affecting the surface quality of the machined components.

Fig. 5(c) shows the rough surface of the machined components at low servo voltage because of increased spark intensity. But, at higher servo voltage, the spark gap widens and reduces the intensity of the spark. This, in turn, increases the flushing and forms the micro cavities on the machined surface leading to a smoother surface of the machined components as shown in Fig. 5(d). From Fig. 5(e), it was observed that a low pulse off time generally offers rough surface on the machined components. That's because, at low pulse off time, cooling time is less which will reduce the amount of molten material to be spilled out from the machining zone and thus forms a rough surface on the machined components.

3.5 Analysis of microstructure

The microstructure of the machined surface of Inconel 706 alloy has been studied based on the image obtained through the scanning electron microscope (SEM) at a magnification of 1,500X. From Fig. 6, it was observed that WED machined surface includes the micro voids, micro globules and melted debris.

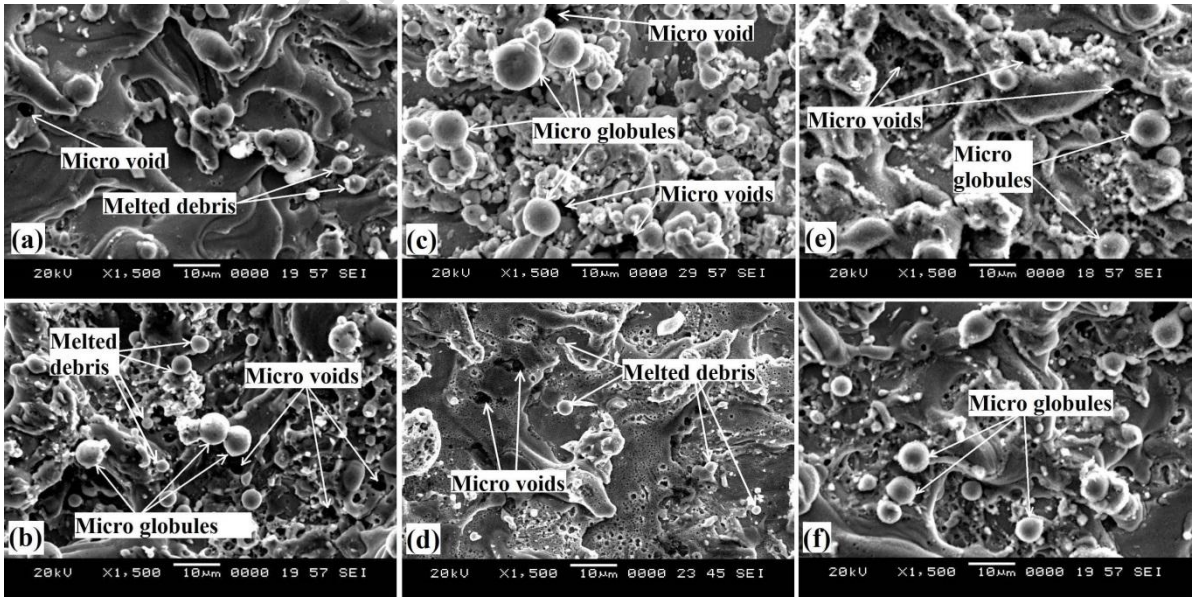

Fig. 6. SEM graph of WED machined surface under the following machine setting: (a) pulse on time of 105 µs; (b) pulse on time of 125 µs; (c) servo voltage of 20 V; (d) servo voltage of 80 V; (e) pulse off time 18 µs; (f) pulse on time 54 µs.

The formation of micro globules is almost similar to the production of powder via atomization of molten material in water. During the electrical discharge, a large volume of

gas is super saturated within the plasma channel. The electrical discharges has the temperature of around 10,000°C which is more than enough to melt and vaporize any conductive material, but it is not sufficient to produce high exploding pressure which can splash all the molten material from the machined surface. When the remaining molten material solidified on the machined surface, some air bubbles get entrapped in the melted region and thus produces micro voids on the machined surface. From Fig. 6(a-b), it was observed that micro globules and micro voids are more prominent at higher pule on time (125 µs) because at higher pulse on time, the amount of thermal energy transferred to the material increases which results in the melting of more amount of material. This, in turn, increases the size of the craters formed on the machined surface and thus produces a rough surface on the machined components.

Similarly, micro voids and micro globules are more prominent at low servo voltage of 20 V as shown in Fig. 6(c). These micro globules and micro voids tend to reduce at high servo voltage of 80 V as shown in Fig. 6(d). This occurs due to an increased gap voltage which tends to increase the spark gap and consequently increases the flushing and thus reduces the growth of micro voids as well as micro globules. From Fig. 6(e), it was evident that micro voids and micro globules are more prominent at pulse off time of 18 µs. Since at low pulse off time, the flushing of melted debris is considerably reduced due to less cooling time and thus allowing the formation of micro voids and micro globules and thus leads to poor surface quality of the machined components. Fig. 6(f) shows that micro voids and micro globules are comparatively reduced at high pulse off time of 54 µs due to increased flushing of melted debris. From Fig. 6(a-f), it was concluded that servo voltage and pulse on time have a significant role to improve the surface features of the machined components. Since micro voids and micro globules are significantly reduced at low pulse on time and high servo voltage.

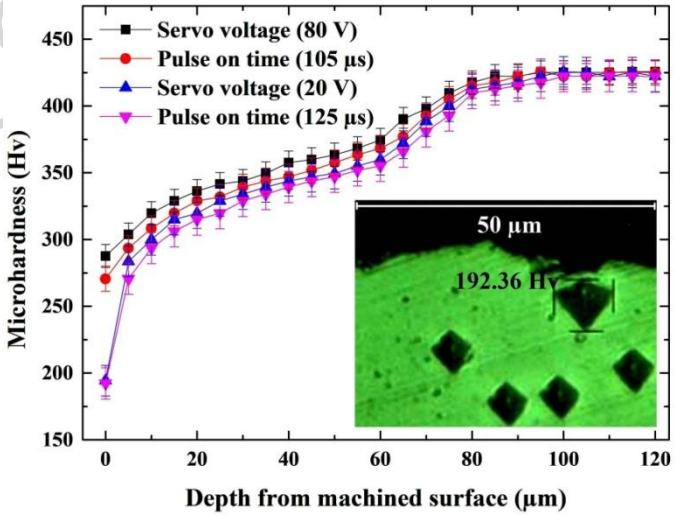

Fig. 7. Subsurface microhardness profile of WED machined components.

3.6 Analysis of microhardness

Fig. 7 shows the cross-sectional view of WED machined surface along with indentations. The nearest region of the machined surface was considered as a reference point (0 µm) since it is extremely difficult to measure the microhardness exactly on the machined edge due to

improper indentations. The indentation nearest to the machined surface is comparatively bigger, but not exactly a rhombus because of metallurgical changes that occurred during the WEDM process. Total 25 measurements were taken in a step of 5 µm till 120 µm and each measurement has been repeated 5 times to enhance the measurement accuracy. The standard error corresponding to each measurement has been indicated in Fig. 7.

The microhardness of WED machined surface was decreased to a certain depth while machining Inconel 706 superalloy. That's because, Inconel 706 includes very low carbon content (wt. 0.06%) which would make the machined subsurface softer after quenching by dielectric fluid. From Fig. 7, it was observed that at high pulse on time of 125 µs and low servo voltage of 20 V, the machined subsurface becomes softer and forms comparatively larger indentation leading to a lower microhardness of the machined components. As a result of WEDM process, the subsurface microhardness of Inconel 706 superalloy was decreased to 192.36 Hv compared to bulk hardness of 425 Hv. The microhardness of subsurface was reduced to a depth of 80 µm due to significant thermal degradation.

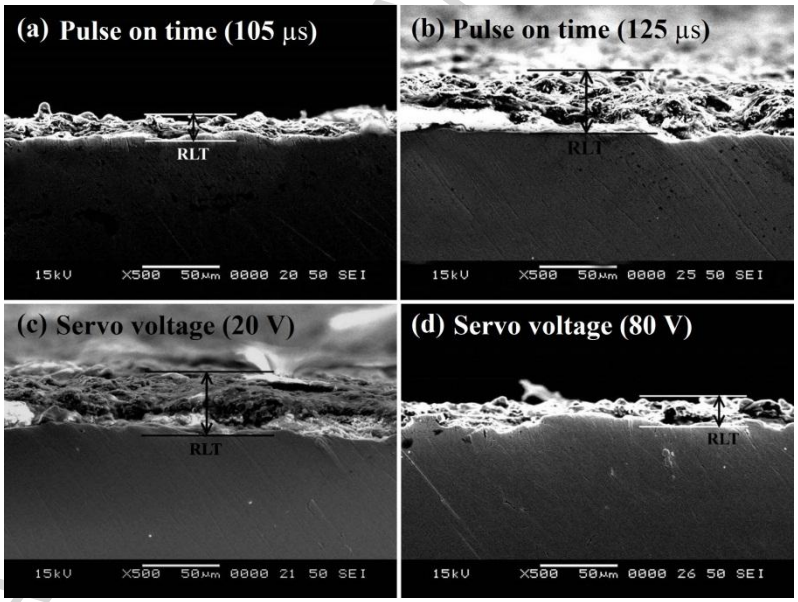

Fig. 8. Recast layer formed on WED machined surface.

3.7 Analysis of recast layer formation

Recast layer is defined as the layer formed on the WED machined surface due to re-solidification of molten material. The recast layer formation may be desirable for some dental applications, but it is detrimental to the aerospace applications. From Fig. 8(b), and Fig. 8(c), it was revealed that the high pulse on time and low servo voltage are the major factors contributing to the recast layer formation. Since, at high pulse on time or low servo voltage, the spark intensity increases and consequently more amount of thermal energy transferred to the material. This, in turn, more amount of molten material resolidify on the machined surface leading to thick recast layer on the machined components. It is essential to minimize the recast layer formation as it creates the metallurgical changes on the machined surface resulting in different material properties. From Fig. 8(a) and Fig. 8(d), it was observed that the average recast layer thickness (RLT) has been reduced significantly at low pulse on time

and high servo voltage because of low spark intensity. In the range of control factors selected, the average RLT was observed within the range of 10 to 50 µm.

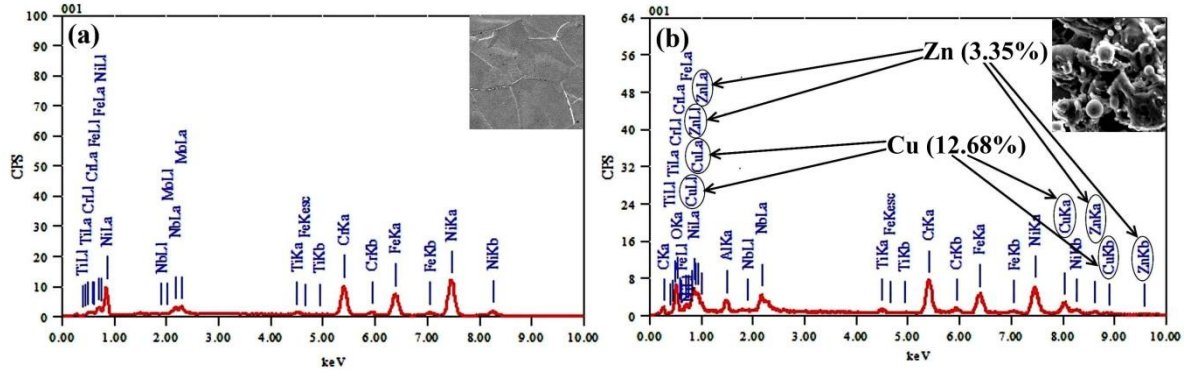

Fig. 9. EDAX analysis of Inconel 706 alloy: (a) polished surface; (b) recast surface.

In the current research work, low hardness of recast layer was observed. This may be due to the fact that the Cu and Zn, which were added to the recast layer during the WEDM process, create the metallurgical changes and exhibit different material properties. Energy dispersive X-ray spectroscopy (EDAX) analysis of recast layer has been shown in Fig. 9(b). The machining conditions such as pulse on time of 125 µs, pulse off time of 36 µs, servo voltage of 50 V, wire feed of 6 m/min, servo feed of 15 mm/min and flushing pressure of 1.96 bar were used to examine the recast surface. Fig. 9(b) indicates the existence of Cu (12.68%) and Zn (3.35%) which was migrated from the brass electrode. In addition, due to rapid heating and cooling during the WEDM operation, the tensile residual stresses may induce within the recast layer and thus reducing the hardness of the recast surface. The relation between hardness and residual stress has been reported in the previous literature [22].

4. Conclusions

The effect of various control parameters such as servo voltage, pulse on time, pulse off time, servo feed, wire feed and flushing pressure on WEDM performance characteristics, namely, MRR and SR of the Inconel 706 alloy components have been investigated. The proposed experimental plan was based on OFAT approach. Moreover, microstructure and surface topography of the machined components have been compared at low and high level of servo voltage, pulse on time, and pulse off time. The microhardness and RLT have been examined using the low and high setting of servo voltage and pulse on time. Furthermore, EDAX analysis has been carried out to study the metallurgical changes on the machined surface. The following conclusions have been drawn based on experimental results:

1. Pulse on time, pulse off time and servo voltage are the major factors influencing the MRR as well as the SR of the machined components whereas the servo feed seems ineffective. The wire feed of 6 m/min and flushing pressure of 1.96 bar have shown the improved MRR as well as SR with the average setting of other control parameters.
2. The SEM analysis revealed that micro globules and micro voids are more prominent at high pulse on time of 125 µs and at low servo voltage of 20 V and thus offers rough surface on the machined components. But, no microcracks were detected on the machined surface due to high toughness of Inconel 706.

3. The surface topography analysis exposed that higher smoothness and fine surface can be obtained on the machined components at low pulse on time of 105 µs, at high servo voltage of 80 V and at high pulse off time of 54 µs using power pulse mode. Whereas, high pulse on time and low servo voltage offer worst surface quality because of high discharge energy during the WEDM process.
4. The subsurface microhardness was decreased to 192.36 Hv due to quenching of dielectric fluid during the WEDM process. Additionally, low carbon content of Inconel 706 would make the machined surface softer. The subsurface microhardness was decreased to a depth of 80 µm due to multiple thermal loading during the WEDM process.
5. The microstructure of the cross section of machined components of Inconel 706 revealed that recast surface is more frequently observed at high pulse on time of 125 µs and high servo voltage of 20 V. The average RLT was found to be within the range of 10 to 50 µm, even though highly variable in nature. Moreover, minimum RLT was obtained at low pulse on time and high servo voltage.
6. The EDAX analysis of recast surface has confirmed the presence of Cu and Zn which causes the metallurgical modifications on machined surface and also shows lowered hardness of the recast region.

Acknowledgements

This work is partially supported by the Department of Science and Technology (DST), Government of India under the project reference number 3802/NITK/MECH/SERB/NS/2014 /A9. The authors would like to thank the DST for its funding support.

References

[1] Pollock, T. M., & Tin, S. (2006). Nickel-based superalloys for advanced turbine engines: chemistry, microstructure and properties. *Journal of propulsion and power*, *22*(2), 361-374.

[2] Zhang, S., & Zhao, D. (Eds.). (2012). *Aerospace Materials Handbook*. CRC Press.

[3] Schilke, P. W., Foster, A. D., & Pepe, J. J. (1991). *Advanced gas turbine materials and coatings*. General Electric Company.

[4] Ezugwu, E. O., Bonney, J., & Yamane, Y. (2003). An overview of the machinability of aeroengine alloys. *Journal of Materials Processing Technology*, *134*(2), 233-253.

[5] Welling, D. (2014). Results of Surface Integrity and Fatigue Study of Wire-EDM Compared to Broaching and Grinding for Demanding Jet Engine Components Made of Inconel 718. *Procedia CIRP*, *13*, 339-344.

[6] Klocke, F., Welling, D., Klink, A., Veselovac, D., Nöthe, T., & Perez, R. (2014). Evaluation of Advanced Wire-EDM Capabilities for the Manufacture of Fir Tree Slots in Inconel 718. *Procedia CIRP*, *14*, 430-435.

[7] Antar, M. T., Soo, S. L., Aspinwall, D. K., Jones, D., & Perez, R. (2011). Productivity and workpiece surface integrity when WEDM aerospace alloys using coated wires. *Procedia Engineering*, *19*, 3-8.

[8] Klocke, F., Welling, D., Klink, A., & Perez, R. (2014). Quality Assessment through In-process Monitoring of Wire-EDM for Fir Tree Slot Production. *Procedia CIRP*, *24*, 97-102.

[9] Atzeni, E., Bassoli, E., Gatto, A., Iuliano, L., Minetola, P., & Salmi, A. (2014). Surface and Sub Surface evaluation in Coated-Wire Electrical Discharge Machining (WEDM) of INCONEL® alloy 718. *Procedia CIRP*, 33, 389-394.

[10] Aspinwall, D. K., Soo, S. L., Berrisford, A. E., & Walder, G. (2008). Workpiece surface roughness and integrity after WEDM of Ti–6Al–4V and Inconel 718 using minimum damage generator technology. *CIRP Annals-Manufacturing Technology*, *57*(1), 187-190.

[11] Newton, T. R., Melkote, S. N., Watkins, T. R., Trejo, R. M., & Reister, L. (2009). Investigation of the effect of process parameters on the formation and characteristics of recast layer in wire-EDM of Inconel 718. *Materials Science and Engineering: A*, *513*, 208-215.

[12] Li, L., Guo, Y. B., Wei, X. T., & Li, W. (2013). Surface integrity characteristics in wire-EDM of Inconel 718 at different discharge energy. *Procedia CIRP*, *6*, 220-225.

[13] Li, L., Wei, X. T., & Li, Z. Y. (2014). Surface integrity evolution and machining efficiency analysis of W-EDM of nickel-based alloy. *Applied Surface Science*, *313*, 138-143.

[14] Antar, M. T., Soo, S. L., Aspinwall, D. K., Sage, C., Cuttell, M., Perez, R., & Winn, A. J. (2012). Fatigue response of Udimet 720 following minimum damage wire electrical discharge machining. *Materials & Design*, *42*, 295-300.

[15] Hewidy, M. S., El-Taweel, T. A., & El-Safty, M. F. (2005). Modelling the machining parameters of wire electrical discharge machining of Inconel 601 using RSM. *Journal of Materials Processing Technology*, *169*(2), 328-336.

[16] Ramakrishnan, R., & Karunamoorthy, L. (2008). Modeling and multi-response optimization of Inconel 718 on machining of CNC WEDM process. *Journal of Materials Processing Technology*, *207*(1), 343-349.

[17] Schilke, P. W., Pepe, J. J., & Schwant, R. C. (1994). Alloy 706 metallurgy and turbine wheel application. Superalloys, 718(625,706), 1.

[18] Technical bulletin: Inconel alloy 706 (Publication number SMC-091), Special Metals Corporation. Received from http://www.specialmetals.com/assets/documents/alloys/inconel/inconel-alloy-706.pdf

[19] Dieter, G. E., & Bacon, D. (1986). *Mechanical metallurgy*. New York: McGraw-Hill, 3, 331-332.

[20] Campbell Jr, F. C. (2011). *Manufacturing technology for aerospace structural materials*. Elsevier.

[21] Okada, A., Konishi, T., Okamoto, Y., & Kurihara, H. (2015). Wire breakage and deflection caused by nozzle jet flushing in wire EDM. *CIRP Annals-Manufacturing Technology*, 64(1), 233-236.

[22] G. Sines & R. Carlson. (1952). Hardness measurement for determination of residual stress. *Bulletin of the American Society of Testing Materials*, 180, 35-37.

Figure caption

Figure No.	Figure Heading
Fig. 1	Profile of WED machined component of Inconel 706 (a); Profile slot obtained after WEDM process (b).
Fig. 2	Microstructure of as-received Inconel 706 (a); and EDAX analysis of Inconel 706 (b).
Fig. 3	Effect of control parameters on MRR.
Fig. 4	Effect of control parameters on SR.
Fig. 5	Surface topography of WED machined surface under the following machine setting: (a) pulse on time of 105 µs; (b) pulse on time of 125 µs; (c) servo voltage of 20 V; (d) servo voltage of 80 V; (e) pulse off time 18 µs; (f) pulse on time 54 µs.
Fig. 6	SEM graph of WED machined surface under the following machine setting: (a) pulse on time of 105 µs; (b) pulse on time of 125 µs; (c) servo voltage of 20 V; (d) servo voltage of 80 V; (e) pulse off time 18 µs; (f) pulse on time 54 µs.
Fig. 7	Subsurface microhardness profile of WED machined components.
Fig. 8	Recast layer formed on WED machined surface.
Fig. 9	EDAX analysis of Inconel 706 alloy: (a) polished surface; (b) recast surface.

Table caption

Table No.	Table Heading
Table 1	Chemical composition of as-received Inconel 706 [18].
Table 2	Physical and mechanical properties of Inconel 706 [18].
Table 3	Control parameters and their levels.
Table 4	Constant process parameters used during the WEDM process.

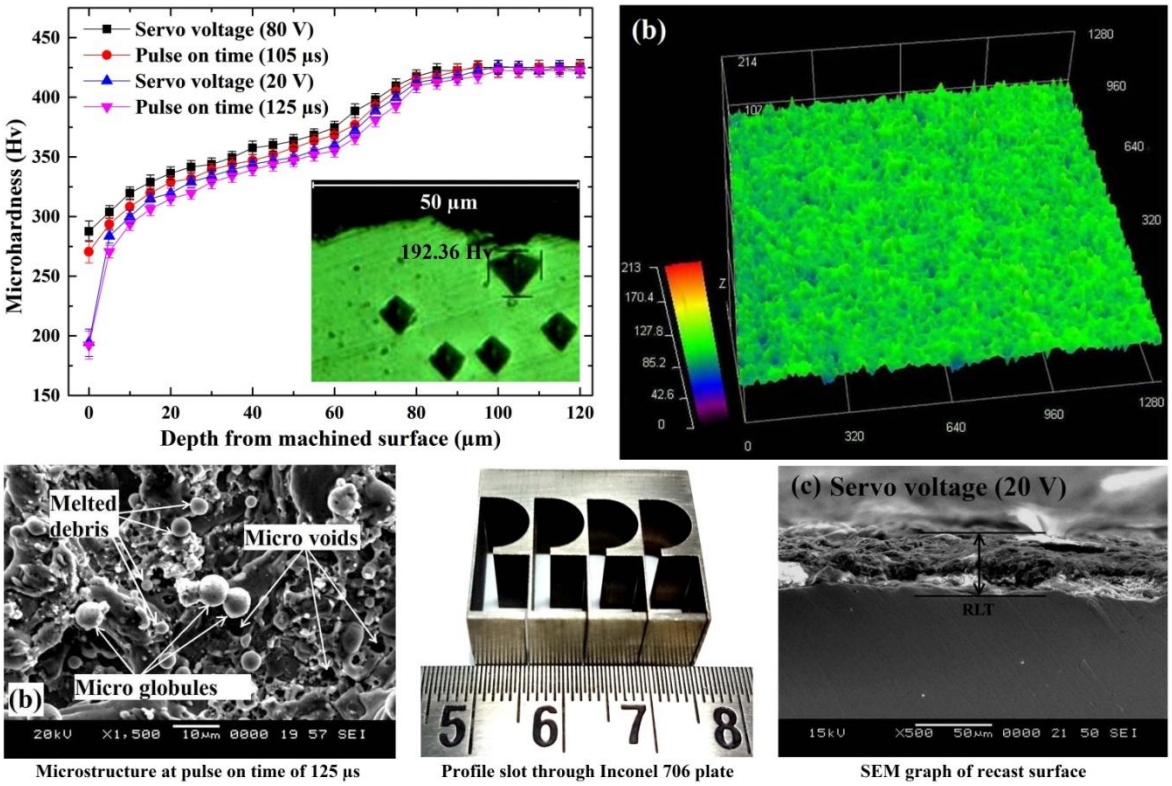

Microstructure at pulse on time of 125 µs | Profile slot through Inconel 706 plate | SEM graph of recast surface

Graphical abstract

Highlights

1. Inconel 706 has been identified as an advanced superalloy as a substitute of Inconel 718 for turbine disk application.
2. Wire electrical discharge machining (WEDM) of Inconel 706 has been done to explore the usages of WEDM for the manufacturing of gas turbine components.
3. Various performance characteristics of WEDM process (i.e., material removal rate, surface roughness, recast layer thickness, microhardness, surface topography, microstructural and metallurgical changes) have been studied to achieve the feasibility in cutting of complex shape profile with high precision through Inconel 706.